C. R. Acad. Sci. Paris, Sciences de la Terre et des planètes / Earth and Planetary Sciences 333 (2001) 557–569

S1251-8050(01)01676-7/FLA

Tectonique / Tectonics

Coulomb interactions and the 17 August 1999 Izmit, Turkey earthquake

Geoffrey C.P. King[a,*], Aurélia Hubert-Ferrari[b], Süleyman S. Nalbant[c], Bertrand Meyer[a], Rolando Armijo[a], David Bowman[a]

[a] Laboratoire de tectonique et mécanique de la lithosphère, Institut de physique du Globe de Paris, 4, place Jussieu, 75252 Paris cedex 05, France
[b] Department of Geoscience, Princeton University, Princeton, NJ 08544, USA
[c] Geophysics Department, Engineering Faculty, Istanbul University, Istanbul, Turkey

Received 26 March 2001; accepted 25 September 2001

Abstract – At 00:02 GMT (03:02 local time) on 17 August, 1999 a magnitude 7.4 (M_s) earthquake occurred 100 km east of Istanbul causing extensive destruction. The event was expected and several scientists have published and attempted to publicize the danger. A paper on stress interactions for NW Turkey (J. Geophys. Res. 103 (1998) 24466–24469) concluded that "by combining the stress change map with the map of active faulting, likely locations for the occurrence of future earthquakes can be refined; faults in the Izmit Bay area, the western part of Biga Peninsula, the Saroz Gulf and a part of western Sea of Marmara must be regarded as posing a specific hazard". An extension of that study is described here. It is shown that the Izmit (1999) earthquake loaded faults both to the east and west of the Izmit rupture. About three months after the Izmit event an M 7.2 earthquake occurred with an epicenter at Duzce extending the Izmit rupture to the east. In the Marmara Sea, west of Izmit, faults have been loaded by between 1 and 5 bar; 5 to 30 % of typical earthquake stress drops in the region suggesting the likelihood of a future event. The risk of a major event on a fault depends not just on stress increases associated with an individual earthquake, but also on the longer-term earthquake history and on tectonic loading. The roles of both are examined over two time periods from 1900 to 1999 and 1700 to 1999. Whatever interpretation we place on the data we conclude that one or two events as great or greater than the recent one is likely to occur within the next few decades near to the northern coast of the Marmara Sea. © 2001 Académie des sciences / Éditions scientifiques et médicales Elsevier SAS

earthquake / active faulting / earthquake probability / Coulomb stress / Turkey

Résumé – Les interactions de la contrainte de Coulomb et le séisme du 17 août 1999 à Izmit en Turquie. À 00:02 GMT (ou 03:02 heure locale), le 17 août 1999, un séisme de magnitude $M_s = 7{,}4$ a détruit la région située à 100 km à l'est d'Istanbul. Cet événement était « attendu », et plusieurs scientifiques avaient dans leurs travaux tenté de prévenir du danger. Un article publié sur les interactions des contraintes dans la région du Nord-Ouest de la Turquie (J. Geophys. Res. 103 (1998) 24466–24469) avait conclu qu'« en combinant les cartes de changement de contraintes avec une carte des failles actives, les lieux probables de futurs grands séismes pouvaient être mieux définis ; les failles de la baie d'Izmit, du golfe de Saros, de l'Ouest de la péninsule de Biga et de la mer de Marmara pouvaient présenter un risque sismique significatif ». C'est une extension de cette étude que nous présentons ici. Il est montré que le séisme d'Izmit de 1999 a augmenté les contraintes sur les failles à l'est et à l'ouest de la rupture d'Izmit. Environ trois mois après le séisme

* Correspondence and reprints.
E-mail addresses: king@ipgp.jussieu.fr (G.C.P. King), ferrari@princeton.edu (A. Hubert-Ferrari).

d'Izmit, un second tremblement de terre, de magnitude 7,2, a frappé la région de Duzce, étendant la rupture d'Izmit plus à l'est. Sur les failles de la mer de Marmara à l'ouest d'Izmit, les contraintes ont augmenté de 1 à 5 bar ; ceci représente 5 à 30 % de la chute de contrainte d'un séisme typique dans la région et suggère donc une forte probabilité de futur séisme sur ces failles. Le risque d'un séisme majeur sur une faille ne dépend pas seulement de l'augmentation de contraintes associée à un séisme individuel, mais aussi de l'histoire sismique à plus long terme. Le rôle de ces deux paramètres est examiné sur deux périodes de temps : 1900–1999 et 1700–1999. Quelle que soit l'interprétation des données, nous concluons qu'un ou plusieurs séismes aussi importants, voire plus, que celui d'Izmit devraient probablement frapper, dans les prochaines décades, la côte nord de la mer de Marmara.

séisme / failles actives / prévision sismique / contrainte de Coulomb / Turquie

1. Introduction

The Marmara Sea region is crossed by the North Anatolian Fault (NAF), which is a 1 600 km long plate boundary that traverses all of northern Turkey [10]. It has hosted many devastating earthquakes both this century and over recorded history [1, 3, 4, 16]. With a slip rate of 2–3 cm·yr^{-1} it is one of the most active strike-slip faults in the world [5, 15, 20, 24]. Our study area extends from 31°0′E, where the North Anatolian fault is a single feature to 26°40′E near the Dardanelle Straits. The fault splits into two main strands 50 km east of Izmit. The northern strand (Northern NAF–NNAF) passes beneath the Sea of Marmara near to its northern coast (and 20 km south of Istanbul) while the southern strand (Southern NAF–SNAF) passes on land to the south of its southern coast. The motion on both strands is predominantly strike-slip with some normal faulting. Normal faulting also occurs beneath the Sea of Marmara. The northern strand is more active than the southern strand [5, 27]. The faults are clearly segmented and three 20th century earthquakes have broken several segments and have fault parameters constrained by instrumental data and the mapping of surface ruptures [21]. The 1912 $M = 7.4$ and 1953 $M = 7.2$ earthquakes are discussed by Nalbant et al. [21]. The recent 17 August 1999 earthquake is discussed below. These events are important to this study since they provide a guide to interpreting earlier $M > 7$ events, in particular how to assess slip on segmented faulting from historical information. It is important to appreciate that the historical data suffer from important limitations. For this reason, it seems that if it is not combined with tectonic studies [e.g. 15 and the later discussion], it can be difficult to draw reasonable conclusions. For example, on the basis of damage alone, Ambraseys and Finkel [3] propose that an earthquake in 1509 ruptured more than 200 km of fault. However, Ambraseys and Jackson [4] propose that no more than 70 km of faulting was involved. In due course improved data from marine tectonic studies together with the damage data will resolve these discrepancies. In this paper we do not include the 1509 event or any other event before. Events since 1700 appear to be well constrained by tectonic and damage information. Similarly we do not pursue the strategy of Parsons, Shinja Toda, Stein, Barka and Dieterich [25] who locate historical events using damage reports alone using the methods of Bakun and Wentworth [8].

The stress coupling between earthquakes follows earlier work where interactions are modeled on the assumption that failure is related to a Coulomb law that includes the effects of both shear and normal stresses (e.g. [18, 19]). We first examine the stress changes due to the Izmit (1999) earthquake and show how it has modified the stress distribution due to earlier events this century. Using these models we discuss the implications for seismic hazard of the transient effects of earthquake stress changes. Tectonic loading is then added, first to the Coulomb interactions this century and then to a catalogue that includes all the events ($M > 6$) since 1700. This allows us to examine the longer-term behavior. The overall of objective our study is to present the information in such a way that its implications and limitations may be easily assessed. This work extends that briefly reported in Nature [15].

2. Coulomb modeling

The stress field due to earthquakes and interseismic loading are calculated using dislocation theory [22]. Dislocations to represent each event or sub-event are approximated by a rectangular plane or planes. The dimensions and locations of each plane must be known plus strike and dip. Slip is defined by amplitude and rake. Places of likely future failure are then identified as having an increased Coulomb Stress ($\Delta\sigma_f$).

$$\Delta\sigma_f = \Delta\tau - \mu' \Delta\sigma_n$$

where $\Delta\tau$ and $\Delta\sigma_n$ are respectively the change in shear and normal stresses on likely future fault planes

and μ' the effective friction. To specify preferred orientations of faulting a regional stress is applied. The direction is more important than the amplitude of the deviatory stress, which is commonly taken to be 100–200 bar. For this paper all fault dislocations extend from the surface to a depth of 15 km. This is slightly greater than the 12.5 km used by Nalbant, Hubert and King [21] and is chosen to be consistent with the loading model (derived from GPS), which favors a locking depth of 15 km.

3. Earthquake interactions since 1900

The Coulomb stress field resulting from all earthquakes this century prior to Izmit (1999) is shown in *figure 1a*. It is modified from Nalbant et al. [21] who examined the evolution of Coulomb stresses for the Sea of Marmara and the Aegean. They showed that 23 out of 29 earthquakes ($M_s \geqslant 6.0$) over an 85-year period could be related to earlier events. Stein, Barkia and Dieterich [26], in a similar study of the North Anatolian fault to the east of our region found that 8 out of the 10 events correlated with earlier events. Taking the two studies together 30 out of 38 events occurred in regions of increased Coulomb stress. All events since 1967 have occurred in regions of enhanced stress, and none have ever occurred in regions of reduced stress. To identify high-risk zones we not only considered regions of increased stress, but also regions of Holocene faulting [14]. It was on this basis that Izmit was identified as a location of high danger (*figure 1a*, plate 2e of [21]). The correlation between events in that study suggests that the effects of interactions can persist for at least 50 years.

The Izmit (1999) earthquake initiated near the town of Golcuk [11, 12]. Coulomb stress in the epicentral region had been increased by between 0.5 and 2.0 bar as a result of previous events and over the last 20 years microseismicity has clustered around the future epicenter (Izinet network determination, Kandilli Observatory). The focal mechanism (Harvard, USGS) was strike-slip consistent with the tectonic environment. Rupture extended for at least 150 km on four main segments with displacements up to 5 m (*figure 1a*) [6, 7, 12]. As a result, the Coulomb stress (*figure 1a*) resolved onto faults west of the rupture rose by 1–5 bar over a distance of 25 km (*figure 1b*) increasing the probability of an earthquake closer to Istanbul. At the eastern end of the rupture, stress was increased by up to 10 bar (*figure 1b*) along the fault, which then ruptured on the 12 November 1999 with up to 5 m of horizontal displacement and locally up to 4 m of vertical displacement. The events have also reduced stress by 3 to 15 bar along 120 km of the SNAF (*figure 1b*) making an event there in the near future less likely.

In *figure 1c* the stress changes due to all $M > 6$ events since 1912 are added. It can be seen that the largest aftershocks (Kandilli Observatory, preliminary locations) fall near to the rupture or at rupture extremities where Coulomb stress was enhanced. The aftershocks are not plotted in *figure 1b*, but it can be seen that the correlation of the aftershocks is better when the earlier seismicity is included (*figure 1c*). The difference between the two figures results mainly from the effects of the 1963 ($M = 6.4$) shock, suggesting that the effects of Coulomb stress changes can last for long periods of time.

4. Tectonic loading

Since the NAF has a high slip rate the effects of tectonic loading should be included. To do this we make the assumption that highly localized shear extends through the lower crust and into the mantle (e.g. [29]). A small amount of (dyke) opening is also allowed. Below a locking-depth deformation is continuous without earthquakes, while above that depth the faulting is seismic. The motion can therefore be modeled by vertical dislocations positioned beneath the mean location of the surface faulting (*figure 2a*). The aesthenosphere is assumed to be ductile. To simulate this, the dislocations are extended to effectively infinite depth. This is equivalent to a dislocation extending to 100 km and a fluid aesthenosphere beneath. The slip parameters for these deep dislocations were established to fit the following criteria. The overall rate should be consistent with recent geological rates (2.0 cm·yr^{-1}) [5, 14] and geodetic rates (3.0 cm·yr^{-1}, [24]) and a reasonable pole of rotation between Europe and Anatolia (29.2°N, 32.9°E, 1.3°·yr^{-1} [14, 20, 24]). They also had to be consistent with the locally measured GPS rates around the Sea of Marmara [27]. *Figure 2a* shows the fits to this data with slip totaling 3.0 cm·yr^{-1} with 0.6 cm·yr^{-1} passing onto the southern branch and 2.4 cm·yr^{-1} on the northern branch. The component of opening on the northern branch that would be consistent with the pole, however, had to be modestly reduced to fit the GPS vectors. The locking depth used was 15 km. It should be appreciated that reasonable fits could also be obtained with locking depths of 10 and 20 km, so these could not be excluded on the grounds that they are inconsistent with the local GPS. However, a locking depth of 10 km seems too small to generate a 7.4 earthquake and 20 km is too big for a region in extension. For a locking depth of 10 km the slip at depth must be dropped to 2.5 cm·yr^{-1} to fit the observations which is possible, but a 20 km locking depth requires it to be increased to nearly 3.5 cm·yr^{-1}, which seems too high. The slip rates that we find are consistent with

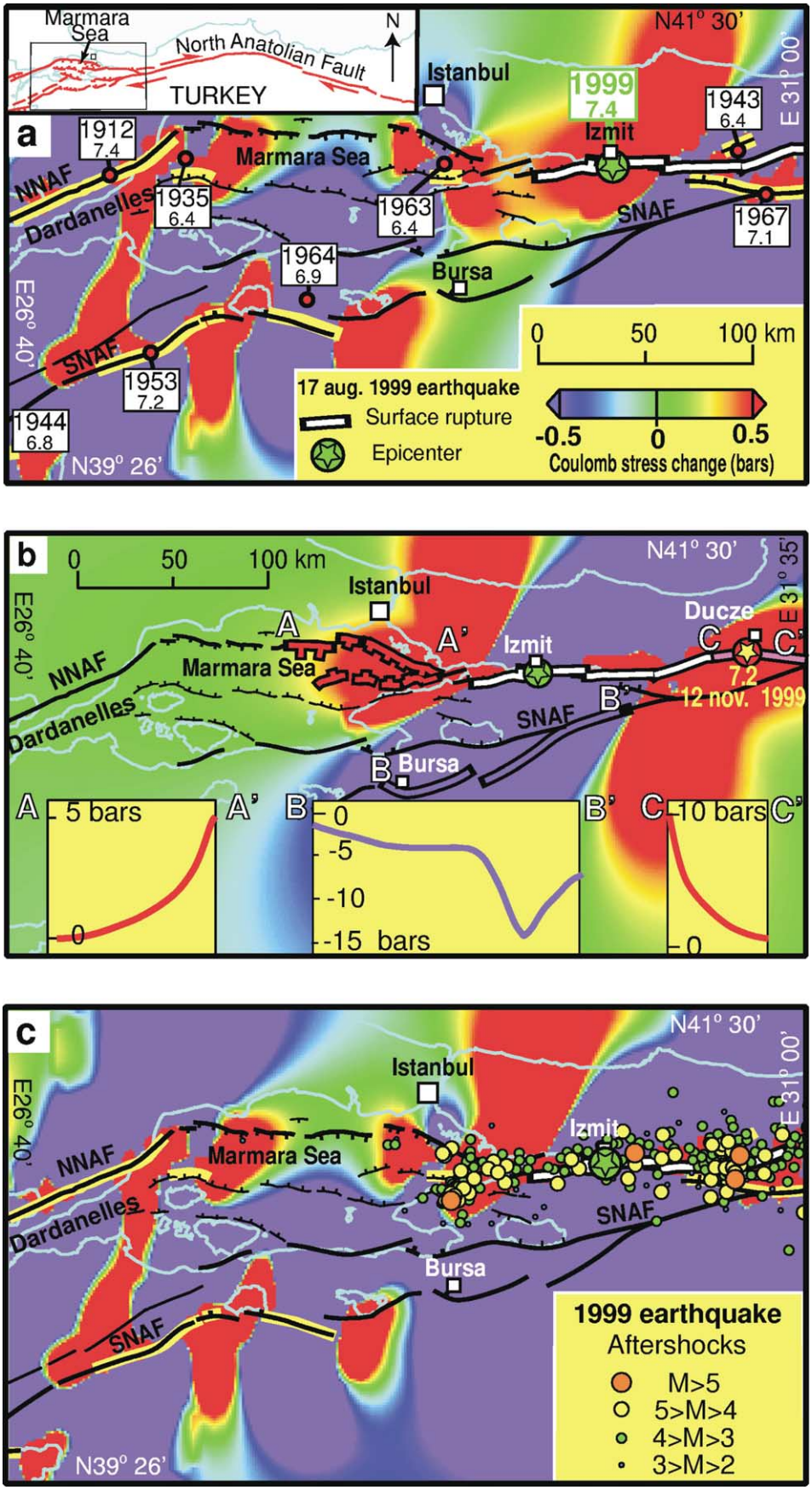
a
Marmara Sea
North Anatolian Fault
TURKEY
N
N41° 30'
E 31° 00'
E26° 40'
N39° 26'
Istanbul
Izmit
Bursa
Marmara Sea
Dardanelles
NNAF
SNAF
1912 7.4
1935 6.4
1963 6.4
1964 6.9
1999 7.4
1943 6.4
1967 7.1
1953 7.2
1944 6.8
0 50 100 km
17 aug. 1999 earthquake
Surface rupture
Epicenter
-0.5 0 0.5
Coulomb stress change (bars)
b
0 50 100 km
N41° 30'
E 31° 35'
E26° 40'
Istanbul
Izmit
Ducze
Marmara Sea
Dardanelles
NNAF
SNAF
Bursa
A
A'
B
B'
C
C'
7.2
12 nov. 1999
5 bars
0
0
-5
-10
-15 bars
10 bars
c
N41° 30'
E 31° 00'
E26° 40'
N39° 26'
Istanbul
Izmit
Bursa
Marmara Sea
Dardanelles
NNAF
SNAF
1999 earthquake
Aftershocks
M>5
5>M>4
4>M>3
3>M>2

the GPS value of Reilinger et al. [24], but higher than the geological rate and the recent GPS [20]. We discuss later in the text the significance for seismic hazard of a reduced slip rate. In *figure 2b*, the stress loading is shown and reaches 0.4 bar·yr^{-1} on the NNAF and 0.1 bar·yr^{-1} on the SNAF.

5. Earthquake interactions and tectonic loading since 1900

In *figure 2c* 100 yr of loading is added to the stress changes due to earthquakes this century prior to Izmit (1999). A high stress region extends along the NNAF from Duzce in the east to the Dardanelles in the west. A more modest stress high extends along the SNAF to the east from Bursa. The apparent hazard on the NNAF is very high over a distance of 300 km indicating the possibility of an $M \approx 8$ earthquake. The Izmit event however ruptured only the eastern 150 km and there is no obvious reason, examining the figure, why rupture should terminate where it did. The stress distribution after the earthquake is shown in *figure 2d*. The NNAF in the Marmara Sea remains highly stressed, but stresses on the SNAF are reduced. Since the time period 1900 to present is short, we have therefore extended the study to include events and loading between 1700 and 1900.

6. Earthquake interactions and tectonic loading since 1700

To generate Coulomb interaction models the rectangular dislocations representing the faults must be defined (fault locations, dimensions, strike and dip). The amplitude and rake of the slip vector must also be specified. For the period 1700 to 1900 these parameters are determined by combining information about damage areas with detailed mapping of Holocene faulting and scaling relations (*table*) [17]. We extend the technique used by Nalbant et al. [21] for earlier events this century and discussed below in Appendix A.

Figure 3a shows the effect of sequential loading of all events from 1719 until before the Izmit (1999) event, and *figure 3b* shows the stress distribution with the Izmit event added. These correspond to *figures 2c* and *2d* for this century, but there are differences. In *figure 3a*, the stressed region where the Izmit earthquake occurred is restricted to 40 km that includes all of the western segment that was the first to rupture in the earthquake. The segments to the east were not uniformly stressed prior to the earthquake and must have become stressed as failure proceeded. Examining the longer time period provides one of the reasons (others are discussed later) for the Izmit (1999) rupture to be limited in its western extent. As for the post-1900 time-period the stress on the SNAF is reduced after the Izmit (1999) earthquake,

Figure 1. a. Coulomb Stress for all events from 1912 to 1983; equivalent to a part of plate 2e of [21]. The fault segments that broke on 17 August 1999 are shown in white. The Coulomb stresses in this new calculation are roughly twice those indicated before (see methods). Towns referred to in the text are added to this figure. **b.** Coulomb stress changes due to the Izmit (1999) earthquake. The event consisted of four on land segments. Rupture may have extended westward beneath the Gulf of Izmit, but this is not modeled here. A segment extends from near Karamursel along the southern coast of the Izmit bay to Golcuk. Stepped to the south at Golcuk, a second segment extends to the northern coast of Lake Sapanca. Again stepped to the south, the third segment extends from the southern shore of the lake to north of Akyasi. The fault then changes strike to form a fourth segment that extends to 15 km southwest of Duzce. Many of the aftershocks fall on or near to regions of enhanced Coulomb stress. The Ducze earthquake epicenter is shown. The two faults west of the new rupture are strongly loaded. The two faults bound the trough 20 km south of Istanbul. The main fault is on the northern side and forms an escarpment 1.2 km high over a distance of 50 km. The inset plots changes of Coulomb stress resolved on the faults **A**–**A′** and **B**–**B′** shown as outlines. The single line in the plot **A**–**A′** corresponds to both of the two outlined faults since they happen to have almost identical stress loading. **c.** Coulomb stress changes due to all events since 1900 plus the Izmit (1999) earthquake. The aftershocks again correlate with the stress changes, but with events notably absent in regions where the 1963 earthquake released stress.

Figure 1. a. Contrainte de Coulomb pour tous les séismes de 1912 à 1983 ; équivalent d'une partie de la plaque 2e [21]. Les segments de faille qui ont rompu le 17 août 1999 sont en blanc. Les contraintes de Coulomb générées par cette nouvelle méthode de calcul représentent approximativement le double de celles d'avant. Les villes auxquelles il est fait référence dans le texte sont ajoutées à la figure. **b.** Changements de la contrainte de Coulomb induites par le séisme d'Izmit de 1999. Ce séisme a rompu quatre segments de faille à terre. La rupture a pu s'étendre plus à l'ouest, sous le golfe d'Izmit, mais ceci n'est pas modélisé ici. Un premier segment s'étend depuis Karamursel, le long de la côte sud de la baie d'Izmit jusqu'à Golcuk. Sautant au sud de Golcuk, un second segment s'étend jusqu'à la côte nord du lac de Sapanca. Sautant à nouveau plus au sud, le troisième segment s'étend du bord sud du lac jusqu'au nord d'Askyasi. La faille change alors de direction pour former un quatrième segment, qui s'arrête à 15 km au sud-ouest de Ducze. Beaucoup de répliques ont eu lieu dans ou près des régions d'augmentation de la contrainte de Coulomb. L'épicentre du séisme de Ducze est indiqué. Sur les deux failles à l'ouest de la nouvelle rupture, les contraintes ont fortement augmenté. Ces deux failles bordent le fossé à 20 km au sud d'Istanbul. La faille principale se situe sur le bord nord et forme un escarpement de 1,2 km de haut sur une distance de 50 km. Les encarts représentent les changements de la contrainte de Coulomb résolus sur les failles **A**–**A′** et **B**–**B′** soulignées. L'unique ligne du graphe **A**–**A′** correspond aux deux failles soulignées, car elles ont subi une augmentation de contrainte presque identique. **c.** Augmentations de la contrainte de Coulomb dues à l'ensemble des séismes depuis 1900, plus le séisme d'Izmit de 1999. Les répliques se corrèlent à nouveau avec les changements de contraintes, mais sont notablement absentes des régions où le séisme de 1963 a relâché les contraintes.

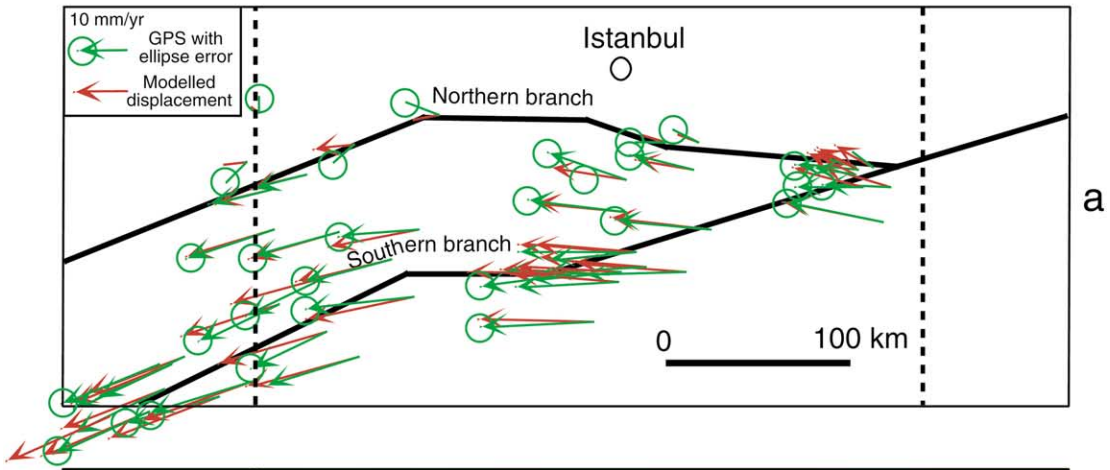

a

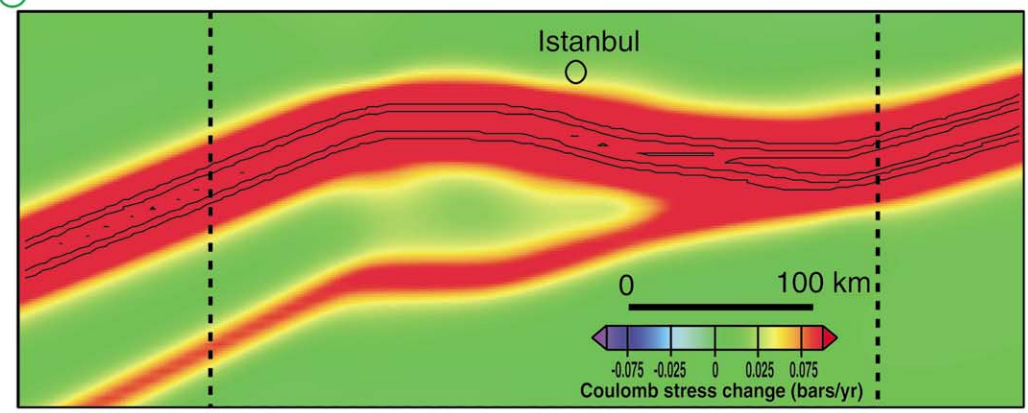

b

1900- before august 1999 loading 15km

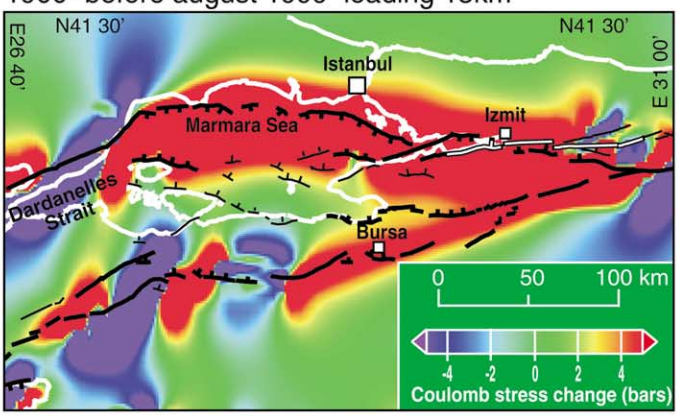

c

1900- after august 1999 loading 15km

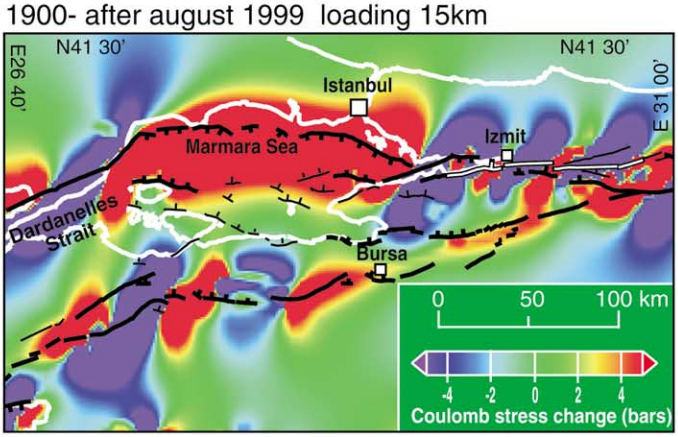

d

but the effect is less pronounced for the longer time period (*figure 3*) than for the shorter period (*figures 2c* and *2d*). This arises because no additional events occur on the SNAF east of Bursa during this 300 yr period.

From the foregoing sections it is clear that, although important detail can be seen when the period is extended, once tectonic loading is added much of the character of the Coulomb Stress distributions (*figures 2b*, *2c* and *3*) is dominated by the larger scale slip deficits. To explore these larger scale features we examine directly slip evolution on the faults. The accumulating slip release due to earthquakes on the NNAF is shown in *figure 4*. *Figure 4a* shows the component of slip resolved parallel to relative plate motion due to all the events to events between 1700 and 1900. Slip is dominated by $M > 7$ events occurring between 1719 and 1766. There are uncertainties in the magnitude of slip of about 1 m and the precise locations of the segments that ruptured in each earthquake cannot be determined unambiguously. However, it seems that taken together they released all the stress previously accumulated. This sequence that propagated from east to west followed events further to the east that ruptured about 500 km of the NAF in 1668. The sequence in which events occurred over this time period is summarized in *figure 4c*.

Following 1766, the stress has again started to accumulate in the Sea of Marmara region. After 146 years when 3.5 m of loading had accumulated, rupture repeated in the west with the 1912 earthquake (*figure 4b*). Then, following major earthquakes further to the east (1939, 1942, 1943 [26]), $M > 7$ earthquakes started to occur in sequence along the eastern part of the Marmara Sea region (1944, 1957, 1967) as shown in *figure 4c*. When this sequence started 5.3 m of loading had accumulated on the NAF as a result of plate motion. The figure also shows the slip due to the Izmit (1999) event, which fills part of the slip deficit that reaches 5.5 m on the NNAF. It is clear why the rupture did not extend further to the east, indeed rupture (including that of the Duzce event) extended into regions for which the historical data do not indicate a slip deficit. However, it is less certain however, why it should not have continued to the west. There are three possible reasons. The first could be that a short term effect due Coulomb stress reduction resulting from the 1963 earthquake (*figure 1a*) may have been sufficient to arrest rupture. The second could be associated with the geometry of faulting. The predominantly strike-slip faults that ruptured in 1719 and 1999 do not extend far into the eastern Marmara Sea. Motion is transferred to fault segments with substantial components of normal slip that bound the trough south of Istanbul. Thus rupture may not readily propagate directly from one fault system to the other. Finally, the Coulomb model based on our understanding of segment geometry and slip history suggests that the rupture may have been arrested by a Coulomb minimum related to earlier events as well as to the 1963 event (*figure 3a*). When the Izmit (1999) event is included, a slip gap remains in the Sea of Marmara over a distance of about 150 km where 5.5 m of slip has accumulated since the 1766.

We do not show a figure for the slip on the SNAF. Unlike the NNAF, the history from 1700 does not provide us with a period when the whole boundary has ruptured. However, major events have occurred west of Bursa and none have occurred to the east in this time period. The resulting stress accumulation can be seen in the Coulomb Stress Coulomb distributions. The last event to have ruptured the eastern part of the fault occurred in 1419. Since then 3.5 m of slip has accumulated over 125 km of the SNAF.

7. Future earthquakes

Various researchers have recently constructed earthquake probabilities of rate state friction based on the

Figure 2. a. The location of the dislocation elements at depth used to provide the loading model. Green arrows are observed GPS slip rates (modified from [27]) with circles indicating approximate errors and red arrows the model fit. **b.** The Coulomb stress loading due to the model shown in **a.** The loading on the northern branch is much greater than for the southern branch. **c.** Coulomb stress distribution with loading from1912 to immediately prior to the Izmit 1999 earthquake. The regions that have enhanced Coulomb stress are similar to those observed in *figure 1a*. The loading however, substantially increases the total Coulomb stress. **d.** Coulomb stress distribution as **c**, but with the Izmit earthquake added. The Coulomb stress is enhanced in the Marmara Sea (as in *figure 1c*), but reduced along the SNAF, which passes through Bursa.

Figure 2. a. Localisation des segments des dislocations utilisés dans le modèle de mise en charge continu des failles en profondeur. Les flèches vertes représentent les vitesses GPS (modifié d'après [27]), les cercles indiquant approximativement les barres d'erreur et les flèches rouges les vitesses prédites par le modèle. **b.** Augmentation de la contrainte de Coulomb due au modèle **a** de mise en charge induite par le modèle. La mise en charge de la branche nord est bien supérieure à celle de la branche sud. **c.** Distributions de la contrainte de Coulomb, avec une mise en charge débutant en 1912 et finissant juste avant le séisme d'Izmit de 1999. Les régions d'augmentation de la contrainte de Coulomb sont similaires à celles de la *figure 1a*. La mise en charge augmente substantiellement, cependant, la magnitude de la contrainte de Coulomb. **d.** Distributions de la contrainte de Coulomb, comme en **c**, mais avec le séisme d'Izmit en plus. La contrainte de Coulomb augmente dans la mer de Marmara (comme sur la *figure 1c*), mais elle est réduite sur la branche sud de la faille Nord-Anatolienne qui passe à Bursa.

Table. Parameters used for the historical seismicity $M \geqslant 6$ between 1700 and 1900. In the absence of tectonic information the slip components on the faults are adjusted such that the horizontal component of slip is parallel to the slip vector between Anatolia and Eurasia. The 1894 event is an exception. As noted above it is thought to be largely normal faulting and be associated with slip partitioning.

Tableau. Paramètres utilisés pour la sismicité historique $M \geqslant 6$ entre 1700 et 1900. En l'absence d'information tectonique, les composantes du glissement sur les failles sont ajustées, de telle manière que le glissement soit parallèle au vecteur glissement entre l'Anatolie et l'Eurasie. Le séisme de 1894 constitue une exception. Comme nous l'avons remarqué ci-dessus, il est associé à une rupture principalement en faille normale, ce qui témoigne d'une séparation entre glissements décrochants et glissements normaux.

Date	M	L (km)	u (m)
25 May 1719	7.6	180	4.5
6 March 1737	7.2	70	2.5
2 September 1754	7.1	45	2.5
22 May 1766a	7.4	110	3.5
5 August 1766b	7.4	130	3.0
29 May 1776	6.3	15	0.5
8 February 1826	6.9	30	2.0
19 April 1850	6.8	25	2.0
28 February 1855	7.4	90	4.0
11 April 1855	6.6	20	1.0
17 September 1857	6.9	30	2.0
6 November 1863	6.9	30	2.0
13 October 1877	6.3	15	0.5
19 April 1878	6.3	15	0.5
26 October 1889	7.0	55	2.0
10 July 1894	7.0	50	2.0

Notes on individual earthquakes identifying the information that was most critical in selecting which fault segments were active

1719 – Destruction extended from Yalova to Duzce (6 000 dead), an area similar to the 1999 Izmit earthquake. However destruction was much greater in Istanbul (many houses and other buildings destroyed, 40 mosques ruined and the city walls badly damaged) so the magnitude seems to have been greater and/or the rupture extended further to the west and closer to Istanbul.

1737 – Heavy destruction with great loss of life on the Biga Peninsula. The earthquake appears to be similar to the 1953 $M = 7.2$ earthquake, but probably on a clear Holocene fault to the north although it could have reactivated the same fault further to the south. The relation to the small 1826 event is not clear, except that the latter was located to the WSW. Both events could be shifted to the WSW along the fault system. Ezine suffered heavy damage although the faulting did not come very close. This may be because of local ground conditions.

1754 – Heavy destruction around the Izmit Gulf (2 000 dead; 60 in Istanbul); heavy damage in Istanbul (collapsed buildings and damage to mosques and the city walls); seismic sea-wave. Location is inferred to be west of the 1719 earthquake and in the Sea of Marmara. As it was less destructive than 1766a its magnitude is assumed to be smaller. Where rupture in this event terminated in the west and rupture in the 1766a began is not certain. We have chosen to separate the two at the clearest segment break judged from the bathymetry. It seems likely that the segment of fault that moved has predominantly normal slip with slip separation between it and the more strike-slip fault passing along the southern side of the Izmit Gulf. In the absence of data to confirm this we have assumed that the horizontal projection of the slip vector is parallel to that predicted by the pole of rotation.

1766a – Heavy damage occurred all around the Sea of Marmara (4 000 dead; 880 in Istanbul) and inland, particularly to the north and west. Large seismic sea-waves. Inferred location is west of the 1754 earthquake and with a greater magnitude. The event may have been smaller than 1719 based on the destruction, but the events were in regions with different population densities. Damage extending to the north and the west is consistent with an east–west propagation of rupture.

1766b – This event added to, and extended westward toward the Dardanelles strait, the destruction due to the previous 1766a earthquake. The inferred location is therefore west of the 1766a event with a magnitude and extent similar to the later 1912 earthquake that occurred in the same area.

1776 – Widespread but minor damage between Gelibolu and Istanbul. The location can only be poorly known for this earthquake, which apparently did not occur close to either the northern or southern coast of the Sea of Marmara. Which of the known fault segments beneath the Marmara Sea moved is not well constrained.

1826 – Destruction and loss of life on the Baya Peninsula and particularly Ezine. Infered location is west of the 1737 earthquake near Ezine.

1850 – Destruction and loss of life near lakes Apolyont and Ulabat. Inferred location is east of the 1737 earthquake and near the 1964 $M = 6.9$ earthquake rupture [21].

1855a – Destruction around the Apolyont Lake (2 000 dead) and Bursa (220 dead in population 35 000). [4] inferred an $M = 7.4$ and we agree with the location of faulting identified by [9].

1855b – Considered as an aftershock of the previous shock, it completed the destruction of Bursa (140 dead) and damaged cities to the north. Inferred location on a fault south of Bursa.

1857 – Damage north east of Bursa, villages between Gemlik and Iznik ruined. Inferred location on the fault segment crossing Gemlik.

1863 – Damage around Lake Iznik. Inferred location east of the previous 1857 earthquake and on the fault bounding the southern shore of the lake.

1877 – Heavy damage in the Marmara Islands. Inferred location and magnitude similar to the 1935 $M = 6.4$ earthquake that occurred in the same area.

1878 – Local damage in the Sapanca-Adapazari area. There is little information to allow this small event to be located on a fault. We have assumed the same fault as the 1943 earthquake.

1894 – Heavy destruction in the Gulf of Izmit between Yalova and Sapanca (990 dead in Sapanca area, 83 in Adapazari and 276 in Istanbul). Seismic sea-wave and the river at Sakarya were diverted. This is the most difficult to place of the larger events (e.g. [2]). The region around Sapanca is complex with multiple faulting and evidence of separation of slip giving faults that are predominantly strike-slip and others with large normal components. In the same region the 1719 event was almost certainly a strike-slip event and the Izmit 1999 event certainly was. These therefore failed to release the extensional component required by the pole of rotation. We therefore place the 1894 event on a major normal fault and provide a substantial component of dip-slip.

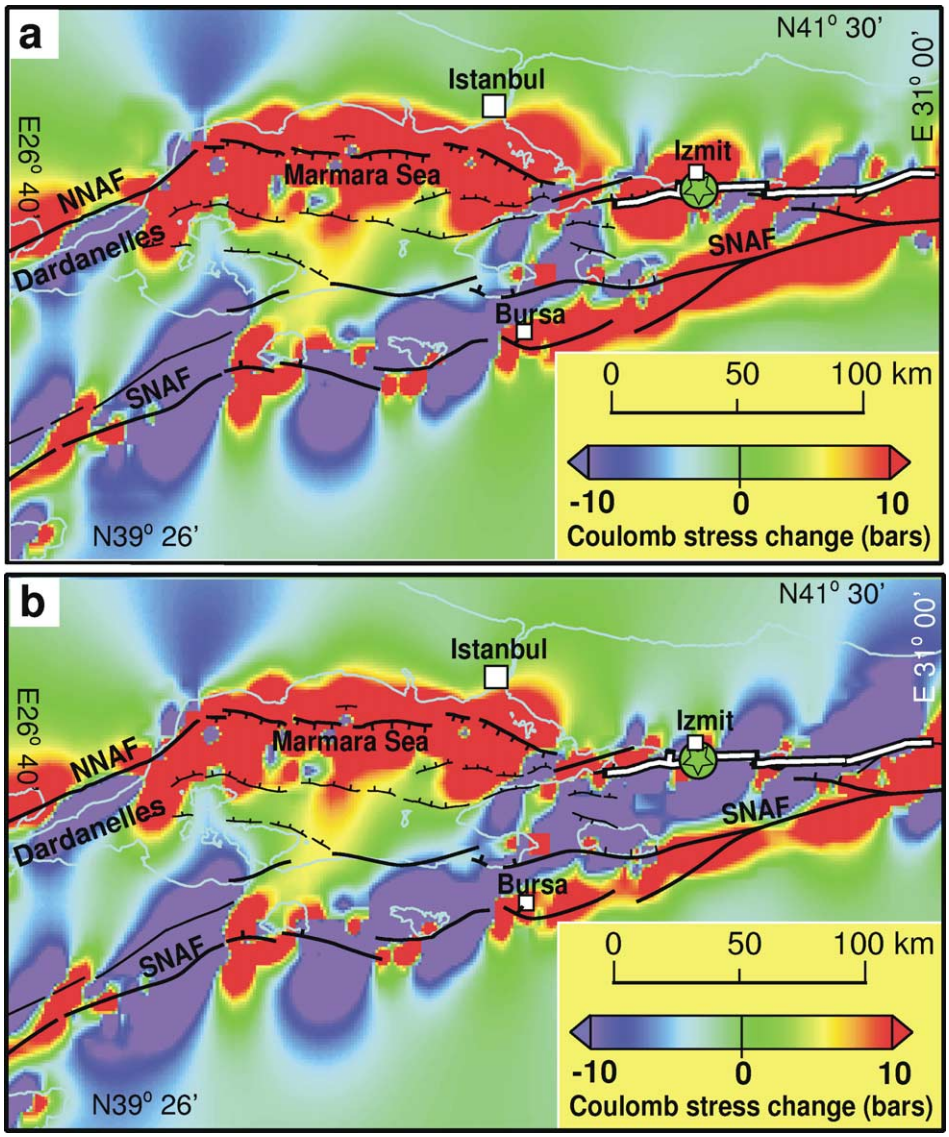

Figure 3. a. Coulomb stress distribution with loading from 1719 to immediately prior to the Izmit 1999 earthquake. The same general regions of high Coulomb stress are identified as are shown in *figure 2d*. However, the highest stress is now localized near the Izmit earthquake epicenter and a region of low Coulomb stress lies between the western part of the Izmit Gulf and the faults further to the west. This region of low stress may have arrested the westward propagation of the Izmit rupture. The longer-term loading increases the stresses for the SNAF passing through Bursa. **b.** Coulomb stress distribution with loading from 1719 including the Izmit 1999 earthquake. The stresses are enhanced for the faulting along the northern coast of the Sea of Marmara. Coulomb stresses along the SNAF passing through Bursa remain high, but are modestly reduced by the earthquake.

Figure 3. a. Distributions de la contrainte de Coulomb avec une mise en charge débutant en 1719 et finissant juste avant le séisme d'Izmit de 1999. En général, les mêmes régions d'augmentation de la contrainte de Coulomb que sur la *figure 2d* peuvent être identifiées. Cependant, la plus forte augmentation de la contrainte de Coulomb est maintenant localisée près de l'épicentre du séisme d'Izmit ; une région contrainte de Coulomb plus faible est située entre la partie ouest du golfe d'Izmit et les failles plus à l'ouest. Cette région de faible contrainte a pu arrêter la propagation vers l'ouest de la rupture d'Izmit. La mise en charge au long terme des failles augmente les contraintes sur la branche sud de la faille Nord-Anatolienne passant par Bursa. **b.** Distributions de la contrainte de Coulomb avec une mise en charge débutant en 1719 et incluant le séisme d'Izmit de 1999. Les contraintes ont augmenté sur les failles le long de la côte nord de la mer de Marmara. Les contraintes de Coulomb le long de la branche sud de la faille Nord-Antolienne passant par Bursa restent fortes, mais sont un peu réduites par le séisme d'Izmit.

concept of rate and state (e.g. [13]) and the ideas have been recently extended [25, 26, 28] as a means of combining earthquake stress changes with other probability estimates. The latter admit that establishing the parameters necessary for such probability evaluations is difficult and while the rate state friction is appealing and provides insight, it may not fully describe the processes involved. For example, crustal fluid flow may be a major effect controlling transient processes (e.g. [23]). The friction laws used in rate-state friction

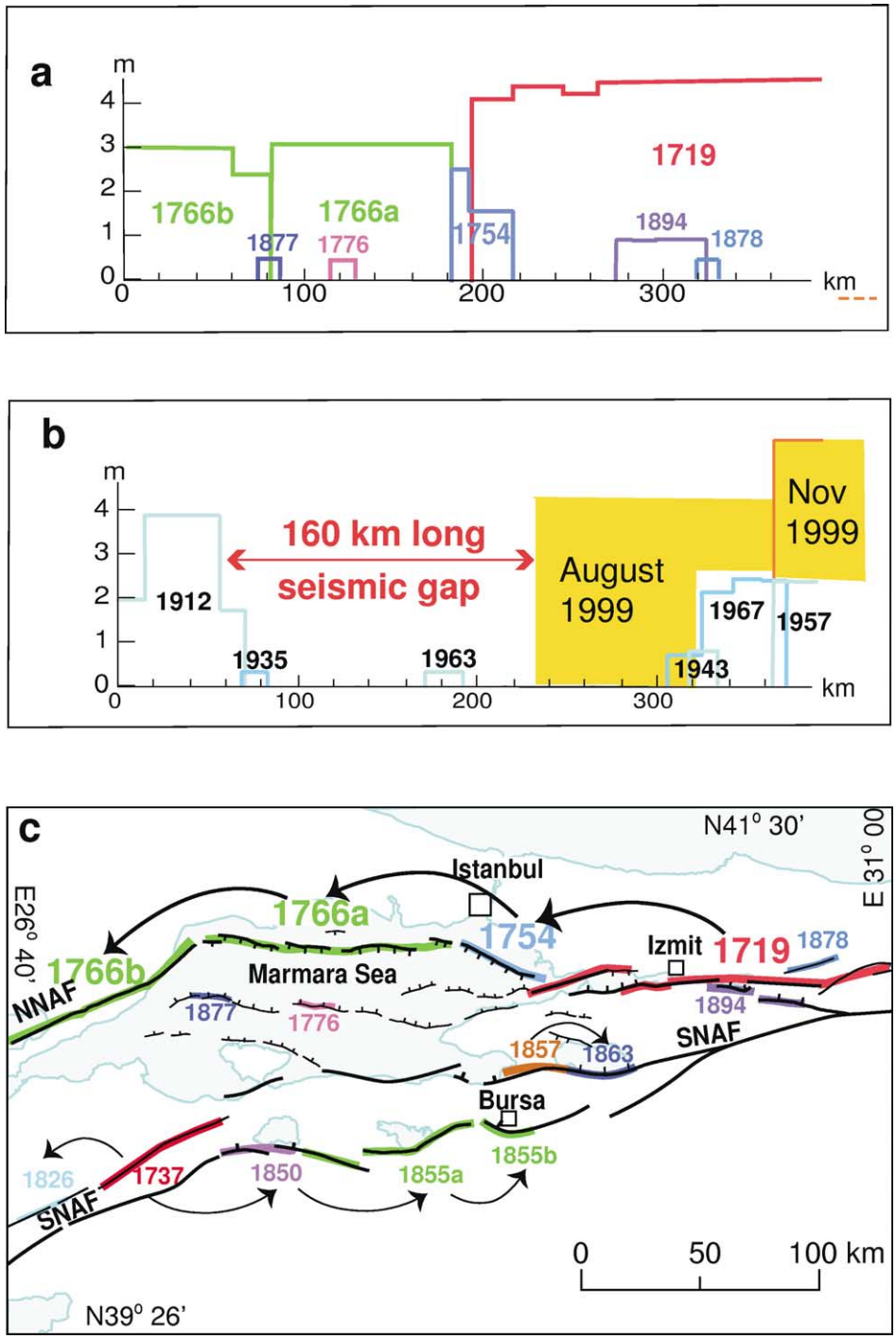

Figure 4. a. Slip for events between 1700 and 1900. The whole Marmara region slipped in the 18th century. Thus by 1766 most of the accumulated slip would have been released. In the preceding century the region east of the 1719 event also slipped (see text). The smaller events contribute little to the total slip. **b.** Slip since 1900. Major events of released slip in the east and west of the Marmara Sea. The slip due to the Izmit (1999) event fills a gap to the east. **c.** The location of fault elements used to model earthquakes between 1700 and 1900. Arrows indicate the overall directions of migration of the events.

Figure 4. a. Glissements associés aux séismes de 1700 à 1900. L'ensemble des failles de la région de Marmara a rompu durant le XVIII^{e} siècle. Ainsi, à partir de 1766, la majeure partie du glissement accumulé a dû être relâchée dans cette région. Durant le siècle précédent, la région à l'est du séisme de 1719 a aussi glissé (voir texte). Les séismes plus petits contribuent peu à l'ensemble du glissement. **b.** Glissements depuis 1900. Les séismes principaux ont eu lieu dans les parties est et ouest de la mer de Marmara. Le glissement associé au séisme d'Izmit de 1999 a rempli un vide existant dans la partie est. **c.** Localisation des segments de failles utilisés pour modéliser les séismes entre 1700 et 1900. Les flèches indiquent la direction générale de la migration des séismes.

models are based on laboratory experiments. Since we still do not fully understand the physics of rock friction, the scaling required to apply these concepts to earthquakes are not well constrained. We therefore consider that while the ideas involved are of major interest and deserve pursuing, we must be cautious about believing numerical predictions of such models [26]. One very useful concept however, is to note that a transient high seismic rate follows a stress step. This is known to occur at the scales of large earthquakes in the form of the aftershock sequence. It is reasonable to assume that, during the aftershock sequence in a region of increased Coulomb Stress, the probability of large event being triggered is greatly increased.

Without considering more complicated concepts, the significance of the observations here can be clarified by discussing the slip deficits and Coulomb stress changes together. A major slip gap (5.5 m) exists on faults beneath the Sea of Marmara that seems to be greater than the slip released by events in 1754 and 1766 following the 1719 earthquake (*figure 4b*). *Figure 1c* shows that faults in the west and east of the Marmara Sea have experienced Coulomb stress increases due to events this century. The stress increase in the west has been present since the 1912 earthquake while that in the east has just happened. In 1719 when an event similar to the Izmit (1999) event occurred, it was followed 35 yr later (in 1754) by an event on a fault to the west. The same fault that has now experienced a Coulomb stress increase (1–5 bar) as a result of the Izmit (1999) event (*figure 1b*). It is therefore likely that this fault will slip again and furthermore, the risk during the aftershock sequence must be regarded as particularly high. Following the 1754 earthquake, the 1766 event ruptured the rest of the fault 12 years later (*figure 4c*). It is likely that a similar sequence will recur. However, since the slip deficit seems greater than that released in the 18th Century, the events that will follow the Izmit (1999) earthquake could occur with shorter time intervals than 35 and 12 yr. Thus not only is the probability of an event within the aftershock period (perhaps 5 yr) likely, an event occurring within 30 yr seems almost certain. A second possibility is that, since the whole fault is primed to slip, it may move in one much larger event. This may be even more probable because, unlike the 1719 to 1766 sequence, the equivalent of the 1766b event (1912) has already occurred. Thus the western part of the fault experiences a Coulomb stress due the 1912 Dardanelles event that did not exist in the previous sequence. If this larger event occurs, it is again probable within 5 yr and nearly certain within 30 yr.

The foregoing scenarios depend on the accuracy of our data and assumptions about the behavior of faults in the Sea of Marmara. It might be supposed that our slip rate of 3 $cm \cdot yr^{-1}$ is too high. However, the earthquake slip that has occurred in the Dardenelles region (3–4 m) and in the west of the Gulf of Izmit (4–5 m) is difficult to explain if the loading rate is less. It is possible that we have over-estimated the slip in these historical earthquakes. If we reduce their slip then the loading slip could also be reduced. We would, in effect, change our scaling laws by reducing the characteristic displacement to length ratio of typical events in the region. In *figure 4* this would be equivalent to changing the vertical scale for the figures. A 2 $cm \cdot yr^{-1}$ slip rate would reduce all slips and slip rates by 2/3. Similar proportional changes apply to stress amplitudes in the Coulomb models. Thus changing the assumed loading rate does not alter our estimate of hazard. The only way to reduce our predicted earthquake hazard would be to assume high creep rates for faults beneath the Sea of Marmara. The fact that these faults have hosted numerous earthquakes throughout history makes this improbable. Paleoseismological studies are needed to provide more information about individual event in this region and to improve Coulomb modeling. However, the very high seismic risk to Istanbul is unlikely to be significantly changed.

Acknowledgements. This work was supported by a Châteaubriand Post-Doctoral Fellowship sponsored by the French Embassy to the United States (DDB), EC Environment Programs (FAUST and PRESAP) and CNRS INSU Grant (contribution number 291). IPGP contribution number 1760.

Appendix A. Fault parameters for earthquakes from 1700 to 1900

All of the $M > 6$ earthquakes in Turkey and the Aegean region produce surface faulting that accumulates to produce morphological features recognizable on detailed sub-areal or bathymetic maps, satellite and aerial photographs and in the field. These allow fault bends, offsets, jogs and other features to be mapped. The faulting can then be divided into segments with characteristic parameters (length, strike, dip and rake). When this information is combined with historical data describing damage, seismic seawaves or liquefaction, all of the parameters of earlier earthquakes can be defined with varying degrees of certainty (*table*). Defining the location of faulting

in the Sea of Marmara is less certain than on land. However any likely modifications as new information becomes available are unlikely to modify the conclusions of this paper.

Historical information for 1700 to 1900 is provided by Ambraseys and Finkel [3] who describe 15 ($M > 6$) in the Marmara region. They separate events into those with $M > 7$ and those with $7 > M > 6$. It seems that all of the $M > 7$ events broke two or more segments while the smaller earthquakes occurred on single segments. Segments associated with an event are initially identified mainly from reported damage. Scaling relations [17] are used to determine magnitude and moment. Slip is then distributed between the dislocations representing the segments.

The final parameters in the *table* are adjusted using two additional criteria. First, if one event was clearly larger than another, its Magnitude should be greater and it should involve a greater length of faulting. Second, unless there is clear evidence that two events occupied the same stretch of fault they are more likely to have occurred on adjacent segments.

An example of the former is provided by the 1719 and 1999 events. Damage in the 1719 occurred in the same places as for the 1999 event. However in 1719 there was severe damage to mosques, the city walls and some major buildings in Istanbul. If such shaking had been repeated in 1999 much greater destruction would have occurred in Istanbul. We therefore conclude that, in addition to the segments that ruptured in 1999, a sub-marine fault segment closer to Istanbul also ruptured in 1719.

An example of the latter is provided by events 1719, 1754, 1766a and 1766b that occurred in a westward migrating sequence from Izmit to the Dardannelle Straits (*figure 4c*). These events are placed such that every segment of this stretch of fault moved once. The location of the 1894 event is also uncertain. We have placed it on a normal fault SE of Izmit rather than supposing that it was a strike-slip event as proposed by Ambraseys [3]. Since there is clear evidence for slip partitioning in this region, this is a reasonable hypothesis. Should the event be made strike-slip, the stress increases in the Sea of Marmara would be even greater than we calculate. The overall conclusions of this paper would not be changed

Defining the slip regions for the six largest events is more straightforward than attributing parameters to some smaller events (1776, 1877, 1850, 1878). There can be a choice of two or even three possible locations separated by up to 20 km. Since these events contribute little to the overall slip however, errors in their location have no significant effect on the conclusions of this paper. The locations of the segments are shown in *figure 4c*.

References

[1] Ambraseys N.N., Some characteristic features of the North Anatolian fault zone, Tectonophysics 9 (1970) 143–165.

[2] Ambraseys N.N., The earthquake of 10 July 1894 in the Gulf of Izmit (Turkey) and its relation to the earthquake of 17 August 1999, Journal of Seismology 5 (2001) 117–128.

[3] Ambraseys N.N., Finkel C., Long-term seismicity of Istanbul and of the Sea Marmara region, Terra Nova 3 (1991) 527–539.

[4] Ambraseys N.N., Jackson J.A., Faulting associated with historical and recent earthquakes in the eastern Mediterranean region, Geophys. J. Int. 133 (1998) 390–406.

[5] Armijo R., Meyer B., Hubert A., Barka A., Westward propagation of the North Anatolian fault into the northern Aegean: timing and kinematics, Geology 27 (1999) 267–270.

[6] Armijo R., Meyer B., Barka A., de Chabalier J.-B., Hubert A., The fault breaks of the 1999 earthquakes in Turkey and the tectonic evolution of the Sea of Marmara: a summary, in: Barka A., Kozaci O., Akyüz S., Altunel E. (Eds.), The 1999 Izmit and Düzce Earthquakes: preliminary results, Istanbul Technical University, Istanbul, 2000, pp. 55–62.

[7] Akyuz S., Hartleb R., Barka A., Altunel E., Sunal G., Meyer B., Armijo R., de Chabalier J.-B., Field observations and slip distribution of the November 12, 1999 Duzce earthquake ($M = 7.1$), Bolu-Turkey, Bull. Seismol. Soc. Am. (submitted).

[8] Bakun W.H., Wentworth C.M., Estimating earthquake location and magnitude from seismic intensity data, Bull. Seismol. Soc. Am. 87 (1997) 1502–1521.

[9] Barka A.A., Kadinsky-Cade K., Strike-slip fault geometry in Turkey and its influence on earthquake activity, Tectonophysics 7 (1988) 663–684.

[10] Barka A.A., The North Anatolian fault zone, Ann. Tectonicae (suppl.) VI (1992) 164–195.

[11] Barka A., The 17 August Izmit earthquake, Science 285 (1999) 1858–1859.

[12] Barka A., Akyuz S., Suna G., Cakir Z., Dikba A., Yerli B., Altunel E., Armijo R., Meyer B., de Chabalier J.-B., Rockwell T., Dolan J., Hartleb R., Dawson T., Christofferson S., Tucker A., Fumal T., Langridge R., Stenner H., Lettis W., Bachuber J., Page W., The August 17, 1999 Izmit earthquake, $M = 7.4$, eastern Marmara region, Turkey: study of surface rupture and slip distribution, Bull. Seismol. Soc. Am. (submitted).

[13] Dieterich J., A constitutive law for rate of earthquake production and its application to earthquake clustering, J. Geophys. Res. 99 (1994) 2601–2618.

[14] Hubert A., La faille Nord-Anatolienne (cinématique, morphologie, localisation, vitesse et décalage total) et modélisations utilisant la contrainte de Coulomb sur differentes échelles de temps, Ph.D thesis, Paris-7 University, Paris, 1998.

[15] Hubert-Ferrari A., Barka A., Nalbant S., Meyer B., Armijo R., Tapponnier P., King G.C.P., Seismic hazard in the Marmara Sea

following the 17 August 1999 Izmit earthquake, Nature (16 March 2000) 269–273.

[16] Hubert-Ferrari A., Armijo R., King G.C.P., Meyer B., Barka A., Morphology, displacement and slip rates along the North Anatolian Fault (Turkey), J. Geophys. Res. (2001).

[17] Kanamori H., Anderson D.L., Theoretical basis of some empirical relations in seismology, Bull. Seismol. Soc. Am. 65 (1975) 1073–1095.

[18] King G.C.P., Cocco M., Fault interaction by elastic stress changes: new clues from earthquake sequences, Adv. Geophys. 44 (2000) 1–38.

[19] King G.C.P., Stein R.S., Lin J., Static stress changes and the triggering of earthquakes, Bull. Seismol. Soc. Am. 84 (1994) 935–953.

[20] McClusky S.C., Balassanian S., Barka A., Demir C., Georgiev I., Hamburger M., Kahle H., Kastens K., Kekelidse G., King R., Kotzev, Lenk O., Mahmoud S., Mishin A., Nadaria M., Ouzounis A., Paradisissis D., Peter Y., Prilepin M., Reilinger R., Sanli I., Seeger H., Teableb A., Toksoz N., Veis, Global Positionning System constraints on plate kinematics and dynamics in the eastern Mediterranean and Caucasus, J. Geophys. Res. 105 (2000) 5695–5719.

[21] Nalbant S.S., Hubert A., King G.C.P., Stress coupling between earthquakes in northwest Turkey and the north Aegean Sea, J. Geophys. Res. 103 (1998) 24466–24469.

[22] Okada Y., Internal deformation due to shear and tensile fault in a half-space, Bull. Seismol. Soc. Am. 82 (1982) 1018–1040.

[23] Noir J., Jacques E., Békri S., Adler P.M., Tapponnier P., King G.C.P., Fluid flow triggered migration of events in the 1989 Dobi earthquake sequence of central Afar, Geophys. Res. Lett. 24 (1997) 2335–2338.

[24] Reilinger R.E., McClusky S.C., Oral M.B., King R.W., Toksoz M.N., Barka A.A., Kinik I., Lenk O., Sanli I., Global Positioning System measurements of the present-day crustal movements in the Arabia-Africa-Eurasia plate collision zone, J. Geophys. Res. 102 (1997) 9983–9999.

[25] Parsons T., Toda S., Stein R.S., Barka A., Dieterich J.H., Heightened odds of a large earthquake near Istanbul: an interaction-based probability calculation, Science 288 (2000) 661–665.

[26] Stein R.S., Barka A.A., Dieterich J.H., Progressive failure on the North Anatolian fault since 1939 by earthquake stress triggering, Geophys. J. Int. 128 (1997) 594–604.

[27] Straub C., Khale H.G., Schindler C., GPS and geological estimates of the tectonic activity in the Marmara Sea region, NW Anatolia, J. Geophys. Res. 102 (1997) 27587–27601.

[28] Toda S., Stein R.S., Reasenberg P.A., Dieterich J.H., Stress transferred by the 1995 $M_w = 6.9$ Kobe, Japan, shock: effect on aftershocks and future earthquake probabilities, J. Geophys. Res. 103 (1998) 24543–24565.

[29] Wittlinger G., Tapponnier P., Poupinet G., Jian Mei, Shi Danian, Herquel G., Masson F.F., Tomographic evidence for localized lithospheric shear along the Altyn Tagh fault, Science 282 (1998) 74–76.